

# Stability and Dynamics of Spike-type Solutions to Delayed Gierer-Meinhardt Equations

N. Khalil      D. Iron      T. Kolokolnikov

October 3, 2018

## Abstract

For a specific set of parameters, we analyze the stability of a one-spike equilibrium solution to the one-dimensional Gierer-Meinhardt reaction-diffusion model with delay in the components of the reaction-kinetics terms. Assuming slow activator diffusivity, we consider instabilities due to Hopf bifurcation in both the spike position and the spike profile for increasing values of the time-delay parameter  $T$ . Using method of matched asymptotic expansions it is shown that the model can be reduced to a system of ordinary differential equations representing the position of the slowly evolving spike solution. The reduced evolution equations for the one-spike solution undergoes a Hopf bifurcation in the spike position in two cases: when the negative feedback of the activator equation is delayed, and when delay is in both the negative feedback of the activator equation and the non-linear production term of the inhibitor equation. Instabilities in the spike profile are also considered, and it is shown that the spike solution is unstable as  $T$  is increased beyond a critical Hopf bifurcation value  $T_H$ , and this occurs for the same cases as in the spike position analysis. In all cases, the instability in the profile is triggered before the positional instability. If however the degradation of activator is delayed, we find stable positional oscillations can occur in this system.

## 1 Introduction

The Gierer-Meinhardt equations are a system of nonlinear reaction-diffusion equations which have been used as a model of organogenesis[7]. The nonlinear terms are used to represent the complex process of protein production regulation. Since this process evolves on a much slower time scale than diffusion and decay, it is natural to consider using delay differential equations when modelling the system. The nonlinear terms are a simplification of a complex series of reactions which may proceed at different rates. In this paper we will consider the effects of delaying various terms in the equations. In each case, we find a reduced system of delayed ordinary differential equations which approximate the behaviour of the full delayed system of partial differential equations. The Gierer-Meinhardt equations, in dimensionless form, without delay are given by,

$$a_t = \epsilon^2 a_{xx} - a + \frac{a^2}{h}, \quad 0 < x < L, t > 0, \quad (1.1a)$$

$$\sigma h_t = Dh_{xx} - \mu h + \frac{a^2}{\epsilon}, \quad 0 < x < L, t > 0. \quad (1.1b)$$

Here  $a$  and  $h$  represent the activator concentration and the inhibitor concentration, respectively. The parameter  $0 < \epsilon \ll 1$  represents the diffusivity of the activator component  $a$ , while the diffusivity of the inhibitor component  $h$  is given by  $D > 0$ , and we assume  $D = O(1)$ . We assume  $\epsilon \ll 1$  so that the activator diffuses more slowly than the inhibitor. The parameters  $0 \leq \sigma \ll 1$  and  $\mu > 0$  represent a time scaling and decay constant for the inhibitor reaction. We have used subscripts to denote partial derivatives. We will use the notation  $a_T = a(x, t - T)$  to represent a delayed term. The exponents in the nonlinear terms correspond to the activator-inhibitor model in the original paper [7]. We have chosen this system to simplify some of the calculations, however, the analysis may be applied to the more general system with some modifications. A key feature of this system is the formation of solutions with spatial structure [10, 11]. In particular,  $a$  will be exponentially small except in well defined regions where the value of  $a$  will be order one. These localized elevated levels of  $a$ , the activator, are thought to cause the localized differentiation of cells in organogenesis.

In [12, 2] the authors consider how delay can enter different terms of the equation. The exact nature of how delay enters the equation can depend on which steps in a complex sequence of reactions are rate limiting steps. We will consider delaying the individual components of the nonlinear reaction terms alone and in combination. We will use similar methods to those considered in [11] to construct a system of delay differential equations approximating the behaviour of the localized spikes in the value of  $a$ . As well we will consider the stability of the slowly evolving spikes. In particular we will consider instability due to Hopf bifurcations occurring as the delay is increased. There are two classes of eigenvalues to consider, referred to as the large and small eigenvalues. The large eigenvalues correspond to profile instabilities and the small eigenvalues correspond to translation instabilities. A Hopf bifurcation occurring in the former will result in spikes which oscillate up and down and in the former spikes which move back and forth. A discussion on the nature and origin of these eigenvalues can be found in [10] and [11].

Simulations of delayed partial differential equations is a relatively new field. Converting the partial differential equation to a system of ordinary differential equations by replacing the Laplacian by a second order centered difference approximation and using `dde23` in Matlab did not provide useful results. The system proved too stiff. A first order implicit-explicit scheme [1] was used instead. The diffusive terms were treated implicitly and the nonlinear terms explicitly. A listing of the code used is given in appendix A. For all simulations of ordinary delayed systems we used the matlab code `dde23` with default settings.

The remainder of this paper will proceed as follows: In §2 we will consider the effect of placing delay in various places in (1.1). In each case the delayed partial differential equation is reduced to a delayed ordinary differential equation for the position of the spike. In §3, we examine the possibility of oscillatory motion of a spike, by finding Hopf bifurcations in the reduced equations for spike position. In §4, we examine Hopf bifurcations in the spike profile. We find that in every case where a Hopf bifurcation occurs in the reduced system, a Hopf bifurcation in the profile has already made the partial differential equation spike solution unstable except in §5, we show that oscillations in spike position is possible for this system if the delay is in the activator degradation.

## 2 Derivation of Differential Equation for Spike Position

We begin by considering the Gierer-Meinhardt Model in (1.1) with fixed delay in some of the nonlinear reaction terms. In each case, we will show that the partial differential equation (PDE) system can be reduced to a system of ordinary differential equations (ODEs) representing the

motion for the corresponding spike solution. Throughout this section we use the method of matched asymptotic expansions and the Van Dyke matching condition in [17] to match the outer and inner asymptotic approximations.

## 2.1 Delay in the Catalyzed Production of Inhibitor

In this section, we will consider the addition of delay to the nonlinear term in (1.1b),

$$a_t = \epsilon^2 a_{xx} - a + \frac{a^2}{h}, \quad 0 < x < L, t > 0 \quad (2.1a)$$

$$0 = Dh_{xx} - \mu h + \frac{a_T^2}{\epsilon}, \quad 0 < x < L, t > 0 \quad (2.1b)$$

$$a_x(0, t) = a_x(L, t) = h_x(0, t) = h_x(L, t) = 0, \quad (2.1c)$$

where  $a_T(x, t) = a(x, t - T)$ . We assume  $0 < \epsilon \ll 1$ , and  $D = O(1)$ . To simplify the analysis we have also assumed  $\sigma = 0$ . The Neumann boundary conditions (2.1c) and assumptions for (2.1) will be used throughout this paper.

In this case the limiting reaction rate step would be in the enhanced production of  $h$  by  $a$ , and therefore we have that the auto-regulation of  $h$  is slow. This is the simplest case we will consider. The methods used in [11] carry over with few changes and the system of differential equations in [11] becomes a system of delayed differential equations here.

We consider a single spike equilibrium solution localized about  $x = x_0$ . We expect the motion of the spike to be on an  $O(\epsilon^2)$  time scale, and therefore we consider the scaling  $\tau = \epsilon^2 t$ . Moreover, we define

$$y = \frac{x - x_0(\tau)}{\epsilon}, \quad \tau = \epsilon^2 t \quad (2.2)$$

as an inner coordinate. With  $y$  as the dependant variable, we use the method of matched asymptotic expansions to construct the equilibrium solution. In the inner region, defined near  $x_0$ , the value of  $h$  is constant to leading order, and the activator concentration is localized. This will allow us to solve for the leading order behaviour of  $a$  in the inner region. In the outer region, away from the spike location  $x_0$ , the activator concentration is exponentially small, and therefore  $a$  will act like a multiple of a Dirac  $\delta$  function. By matching the inner and outer regions, we will construct the leading order solution to  $h$  in the outer region. The second order equations will then result in a solvability condition which results in an equation governing the motion of the spike.

In the inner region, we introduce the new variables

$$a(x) = a(x_0 + \epsilon y) = A(y); \quad h(x) = h(x_0 + \epsilon y) = H(y). \quad (2.3)$$

Thus the model in (2.1) becomes

$$-\epsilon A_y \dot{x}_0 = A_{yy} - A + \frac{A^2}{H}, \quad -\infty < y < \infty \quad (2.4a)$$

$$0 = \frac{D}{\epsilon^2} H_{yy} - \mu H + \frac{A_T^2}{\epsilon}, \quad -\infty < y < \infty \quad (2.4b)$$

where  $A_T = A(y, \tau - \epsilon^2 T)$ , and  $x_0 = x_0(\tau)$ .

Using the expansion  $A(y) = A_0(y) + \epsilon A_1(y) + \dots$  and  $H(y) = H_0(y) + \epsilon H_1(y) + \dots$ , we get that, to leading order in  $\epsilon$ ,

$$0 = A_{0yy} - A_0 + \frac{A_0^2}{H_0}, \quad (2.5a)$$

$$0 = DH_{0yy} \implies H(y) \approx H_0 = \text{constant}. \quad (2.5b)$$

Next, we introduce  $w(y)$  and we rescale  $A_0 = H_0 w(y)$ . Then equation (2.5a) simplifies to

$$\begin{cases} w'' - w + w^2 = 0, & -\infty < y < \infty \\ w(y) \rightarrow 0 \text{ as } |y| \rightarrow \infty; & w'(0) = 0; \quad w(0) > 0, \end{cases} \quad (2.6)$$

whose solution is the unique positive homoclinic curve

$$w(y) = \frac{3}{2} \operatorname{sech}^2\left(\frac{y}{2}\right). \quad (2.7)$$

Thus,  $a(x) = H_0 w\left(\frac{x - x_0(\tau)}{\epsilon}\right)$  looks like a spike near  $x = x_0$ . Moreover, the inner expansion of the variables in (2.23b), gives the  $O(\epsilon)$  equation

$$A_{1yy} - A_1 + 2\frac{A_0}{H_0}A_1 = -\dot{x}_0 A_{0y} + \frac{A_0^2}{H_0}H_1. \quad (2.8)$$

The right hand side of (2.8) must be orthogonal to the homogeneous solution  $A_{0y}$  of (2.8) under the dot product  $u \cdot v = \int_{-\infty}^{\infty} uv \, dy$ . From this solvability condition, we get the motion equation

$$-\dot{x}_0 A_{0y} = -\frac{A_0^2}{H_0}H_1. \quad (2.9)$$

Multiplying both sides of equation (2.9) by  $A_{0y}$  and integrating by parts twice gives

$$-\dot{x}_0 \int_{-\infty}^{\infty} (A_{0y})^2 \, dy = \frac{1}{3H_0^2} \left( \int_{-\infty}^{\infty} A_0^3 \, dy \right) (H_{1y}(\infty) + H_{1y}(-\infty)), \quad (2.10)$$

where we have used the fact that  $H_{1yy}$  is an even function.

In the outer region, since  $w \rightarrow 0$  as  $y \rightarrow \pm\infty$ , therefore we have that  $a \rightarrow 0$  for  $|x - x_0| \gg \epsilon$ . Also, for  $\epsilon \ll 1$ , we ignore the  $\epsilon^2 a_{xx}$  term in (2.1), and the model reduces to

$$\begin{cases} -a + \frac{a^2}{h} = 0, & 0 < x < L, \\ Dh'' - \mu h + \frac{a_T^2}{\epsilon} = 0, & 0 < x < L, \end{cases}$$

which implies that

$$a \equiv 0; \quad \text{and} \quad \begin{cases} Dh'' - \mu h = -\frac{a_T^2}{\epsilon}, & 0 < x < L, \\ h'(0) = h'(L) = 0, \end{cases} \quad (2.11)$$

where we note that  $h'(x)$  is discontinuous at  $x = x_0$ .

To find  $h$ , we treat  $a$  as a multiple of the Dirac delta function, and we match to the inner variables. We expand  $h = h_0 + \dots$ , where  $h_0$  satisfies

$$\begin{cases} Dh_0'' - \mu h_0 = \beta \delta(x - x_0(\tau - T)), & 0 < x < L, \\ h_0'(0) = h_0'(L) = 0, \end{cases} \quad (2.12)$$

where  $\beta$  is defined by

$$\beta = \int_{-\infty}^{\infty} A_0^2(y) dy. \quad (2.13)$$

We can therefore solve for  $h_0$  in (2.12) by introducing the Green's function  $G(x; x_0)$  satisfying

$$\begin{cases} DG_{xx} - \mu G = -\delta(x - x_{0T}), & 0 < x < L, \\ G_x(0; x_0) = G_x(L; x_0) = 0. \end{cases} \quad (2.14)$$

To simplify the notation, we assume  $\mu = 1$  and  $D = 1$  and let the length of the domain,  $L$ , vary. Thus, we get

$$G(x; x_{0T}) = \frac{1}{\sinh(L)} \begin{cases} \cosh(x) \cosh(x_{0T} - L), & 0 < x < x_0, \\ \cosh(x_{0T}) \cosh(x - L), & x_0 < x < L, \end{cases} \quad (2.15)$$

where  $G(x; x_{0T}) = G(x; x_0(\tau - T))$ .

In terms of the Green's function, the solution to (2.12) is

$$h_0 = \beta G(x; x_{0T}). \quad (2.16)$$

Moreover, since  $A_0 = w(y)H_0$  where  $H_0$  is the value of  $h_0$  in the inner region, therefore  $H_0$  can be determined by matching the inner and outer regions. This gives that

$$H_0 = h_0(x_0) = \beta G(x_0; x_{0T}). \quad (2.17)$$

Substituting (2.17) into (2.10) gives

$$-\dot{x}_0 \int_{-\infty}^{\infty} (A_{0y})^2 dy = \frac{1}{6\beta} \left( \int_{-\infty}^{\infty} A_0^3 dy \right) \left( \frac{G_x^- + G_x^+}{G^2(x_0; x_{0T})} \right). \quad (2.18)$$

Solving for  $\dot{x}_0$  in (2.18), and simplifying yields the ODE

$$\dot{x}_0 = -\frac{G_x^- + G_x^+}{G(x_0; x_{0T})}. \quad (2.19)$$

From (2.15), we get that

$$G_x^- = G_x(x_0^-; x_{0T}) = \frac{\cosh(x_{0T} - L) \sinh(x_0)}{\sinh(L)}; \quad (2.20a)$$

$$G_x^+ = G_x(x_0^+; x_{0T}) = \frac{\cosh(x_{0T}) \sinh(x_0 - L)}{\sinh(L)}. \quad (2.20b)$$

Reverting back to the initial time scale and substituting (2.15) and (2.20) into (2.19) yields the ordinary differential equation for the motion of the spike described by

$$\frac{dx_0}{dt} = -\epsilon^2 \left( \frac{\cosh(x_{0T} - L) \sinh(x_0) + \cosh(x_{0T}) \sinh(x_0 - L)}{\cosh(x_0 - L) \cosh(x_{0T})} \right). \quad (2.21)$$

We remark that for  $T = 0$  the equilibrium equation in (2.21) has similar terms to the one derived in [11] for the model without delay. In figure 1, we assume  $x_0 = .5$  and  $L = 1$ , and we compare the full numerical simulation as obtained from (2.1) with the asymptotic result obtained by solving (2.21) for  $x_0(t)$ . We find a close agreement between the two results.

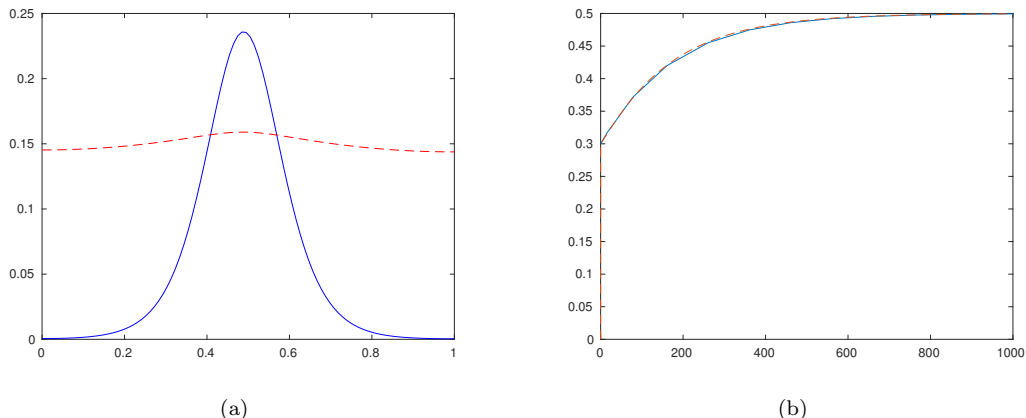


Figure 1: Left: Plot of the one-spike stable equilibrium solution  $a$  (solid curve) and  $h$  (dotted curve) for the model in (2.1) with delay in the inhibitor equation. Right: Plot of the trajectory  $x_0(t)$  for the center of the spike. The dotted curve is the full numerical simulation obtained from (2.1), and the solid curve is the asymptotic result as obtained from (2.21), with delay in the non-linear term of the inhibitor equation. Parameter values used are  $T = 0.1$ ,  $\epsilon = 0.06$ ,  $\mu = 1$ ,  $L = 1$  and  $D = 1$ .

## 2.2 Delay in the Regulation of Activator Production

In this section we analyze the model in (1.1) with delay in the nonlinear term of the activator equation, and thus the rate limiting step would be in the negative feedback process. In §2.4 we consider delaying the entire term, but this analysis is more involved. The partial differential equations for the model are

$$a_t = \epsilon^2 a_{xx} - a + \frac{a^2}{h_T}, \quad 0 < x < L, t > 0 \quad (2.22a)$$

$$0 = Dh_{xx} - \mu h + \frac{a^2}{\epsilon}, \quad 0 < x < L, t > 0 \quad (2.22b)$$

with the same assumptions and boundary conditions as in Section 2.1. The analysis here is similar to the one in §2.1, however we note that in this case even a small delay will result in significant changes in the behaviour of the system. Using the dependant variable  $y$ , as defined in (2.2), we use

the method of matched asymptotic expansions to construct the equilibrium solution. As before, the value of  $h$  is constant to leading order in the inner region, and we solve for the leading order behaviour of  $a$ . In the outer region, we again treat  $a$  as a multiple of a Dirac  $\delta$  function, and we construct the leading order solution to  $h$  in the outer region, and use it to find an equation governing the motion of the spike.

In the inner region, the model in (2.22) written in terms of the inner variables becomes

$$-\epsilon A_y \dot{x}_0 = A_{yy} - A + \frac{A^2}{H_T}, \quad -\infty < y < \infty \quad (2.23a)$$

$$0 = \frac{D}{\epsilon^2} H_{yy} - \mu H + \frac{A^2}{\epsilon}, \quad -\infty < y < \infty \quad (2.23b)$$

where  $H_T = H(y, \tau - T)$ ,  $x_0 = x_0(\tau)$ , and  $\tau = \epsilon^2 t$ . Using an inner expansion for  $A(y)$  and  $H(y)$ , and rescaling  $A_0 = H_{0T} w(y)$ , yields the system in (2.6), with the unique solution  $w(y)$  in (2.7). Also, the next order expansion is simplified using the solvability condition, and we get

$$-\dot{x}_0 A_{0y} = -\frac{A_0^2}{H_{0T}} H_{1T}. \quad (2.24)$$

Multiplying both sides of equation (2.24) by  $A_{0y}$  and integrating by parts twice gives

$$-\dot{x}_0 \int_{-\infty}^{\infty} (A_{0y})^2 dy = \frac{1}{3H_{0T}^2} \left( \int_{-\infty}^{\infty} A_0^3 dy \right) (H_{1yT}(\infty) + H_{1yT}(-\infty)). \quad (2.25)$$

In the outer region, the model in (2.22) reduces to

$$\begin{cases} -a + \frac{a^2}{h_T} = 0, & 0 < x < L, \\ Dh'' - \mu h + \frac{a^2}{\epsilon} = 0, & 0 < x < L, \end{cases}$$

and we get

$$a \equiv 0; \quad \text{and} \quad \begin{cases} Dh'' - \mu h = -\frac{a^2}{\epsilon}, & 0 < x < L \\ h'(0) = h'(L) = 0 \end{cases} \quad (2.26)$$

where  $h'(x)$  has a jump discontinuity at  $x = x_0$ . Using the expansion  $h = h_0 + \dots$  while treating  $a$  as a multiple of the Dirac delta function, and matching to the inner solution gives

$$Dh_0'' - \mu h_0 = \beta \delta(x - x_0(\tau)), \quad \text{where} \quad \beta = \int_{-\infty}^{\infty} A_0^2(y) dy. \quad (2.27)$$

with the same boundary conditions as (2.12). In terms of the Green's function (2.15), the solution  $h_0$  for the system in (2.27) is given by

$$h_0 = \beta G(x; x_0), \quad (2.28)$$

and thus we get that

$$H_{0T} = h_{0T} = \beta G(x_{0T}; x_{0T}). \quad (2.29)$$

Substituting (2.29) into (2.25) and simplifying gives

$$\dot{x}_0 = -\frac{G_{x_T}^- + G_{x_T}^+}{G(x_{0T}; x_{0T})}, \quad (2.30)$$

where

$$G_{x_T}^- = G_x(x_{0T}^-; x_{0T}) = \frac{\cosh(x_{0T} - L) \sinh(x_{0T})}{\sinh(L)}, \quad \text{and} \quad (2.31a)$$

$$G_{x_T}^+ = G_x(x_{0T}^+; x_{0T}) = \frac{\cosh(x_{0T}) \sinh(x_{0T} - L)}{\sinh(L)}. \quad (2.31b)$$

Thus, in terms of the initial time scale we get

$$\frac{dx_0}{dt} = -\epsilon^2 \left( \frac{\sinh(2x_{0T} - L)}{\cosh(x_{0T} - L) \cosh(x_{0T})} \right). \quad (2.32)$$

We observe that delay appears in every term of (2.32), which results in considerably different dynamics than the one derived in §2.1. Numerical simulations of this system are carried out and analyzed in figure 2. We find that even a small delay will have a significant effect on the dynamics, and we also show that a Hopf bifurcation occurs at some critical values of the delay  $T$ .

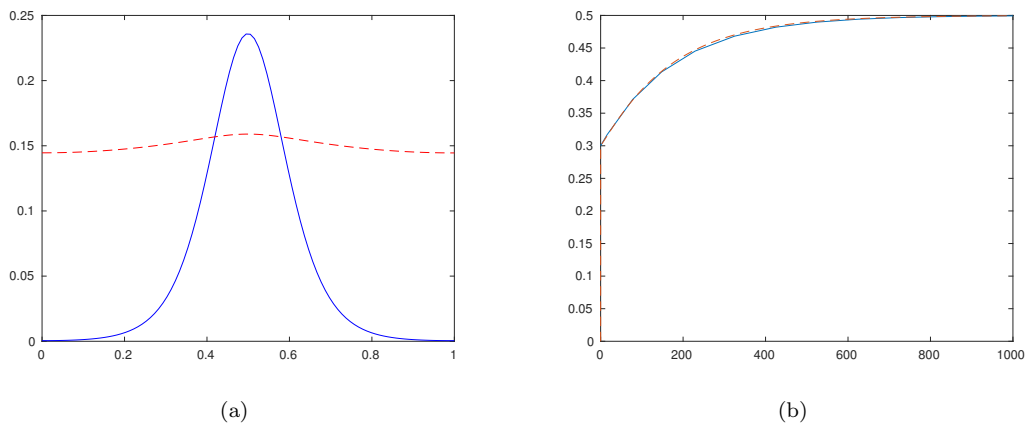


Figure 2: Left: Plot of the one-spike stable equilibrium solution  $a$  (solid curve) and  $h$  (dotted curve) for the model in (2.22), with delay in the  $h$  term of the activator equation. Right: Plot of the trajectory  $x_0(t)$  for the center of the spike. The dotted curve is the full numerical simulation obtained from (2.22), and the solid curve is the asymptotic result as obtained from (2.32), with delay in the  $h$  term of the activator equation. Parameter values used are  $T = 0.1$ ,  $\epsilon = 0.06$ ,  $\mu = 1$ ,  $L = 1$  and  $D = 1$ .

### 2.3 Delay in Activator Regulation and Inhibitor Production

Next, we consider the following model with delay in the nonlinear terms of both equations:

$$a_t = \epsilon^2 a_{xx} - a + \frac{a^2}{h_T}, \quad 0 < x < L, t > 0 \quad (2.33a)$$

$$0 = Dh_{xx} - \mu h + \frac{a_T^2}{\epsilon}, \quad 0 < x < L, t > 0 \quad (2.33b)$$

with the same boundary conditions and assumptions as before.

In the inner region, we again introduce the new variables (2.2) and (2.3) into (2.33), and we get

$$-\epsilon A_y \dot{x}_0 = A_{yy} - A + \frac{A^2}{H_T}, \quad |y| < \infty, \quad (2.34a)$$

$$0 = \frac{D}{\epsilon^2} H_{yy} - \mu H + \frac{A_T^2}{\epsilon}, \quad |y| < \infty. \quad (2.34b)$$

Using the inner expansion for  $A(y)$  and  $H(y)$ , and rescaling  $A_0 = H_{0T} w(y)$ , gives (2.6) with the unique solution (2.7). Moreover, we get (2.25) for the next order expansion.

In the outer region, where  $w \rightarrow 0$  as  $y \rightarrow \pm\infty$ , we have

$$\begin{cases} -a + \frac{a^2}{h_T} = 0, & 0 < x < L, \\ Dh'' - \mu h + \frac{a_T^2}{\epsilon} = 0, & 0 < x < L, \end{cases}$$

which implies that

$$a \equiv 0; \quad \text{and} \quad \begin{cases} Dh'' - \mu h = -\frac{a_T^2}{\epsilon}, & 0 < x < L, \\ h'(0) = h'(L) = 0, \end{cases} \quad (2.35)$$

where  $h'(x)$  is discontinuous at  $x = x_0$ . Using the Green's function in (2.15), together with the solution  $h_0$  in (2.16), and the expression (2.17) for  $H_0$ , give that

$$H_{0T} = h_0(x_{0T}) = \beta G(x_{0T_1}; x_{0T_2}), \quad (2.36)$$

where  $x_{0T_1} = x_0(\tau - T)$ , and  $x_{0T_2} = x_0(\tau - 2T)$ . Substituting (2.36) into (2.25) gives

$$\dot{x}_0 = -\frac{G_x^-(x_{0T_1}; x_{0T_2}) + G_x^+(x_{0T_1}; x_{0T_2})}{G(x_{0T_1}; x_{0T_2})}. \quad (2.37)$$

Therefore, for  $0 < x < L$ , using the initial time scale we get the following asymptotic ODE for the position of the spike:

$$\frac{dx_0}{dt} = -\epsilon^2 \left( \frac{\sinh(x_{0T_1} + x_{0T_2} - L)}{\cosh(x_{0T_1} - L) \cosh(x_{0T_2})} \right). \quad (2.38)$$

Similar to the previous result in (2.32), we have delay appearing in every term of the quasi-equilibrium equation (2.38), but with two different values. In §3, we numerically analyze the

stability of the equilibrium solution for the spike position obtained from (2.38) and we compare these results to the full numerical simulation for the corresponding PDE system in (2.33).

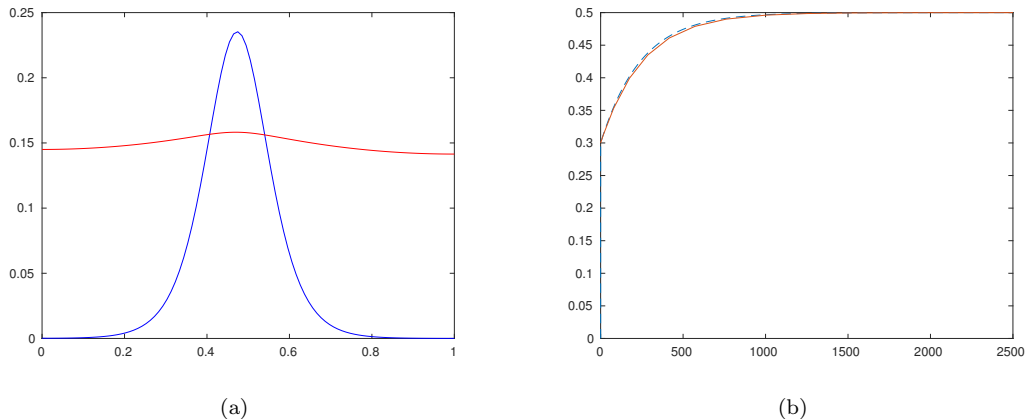


Figure 3: Left: Plot of the one-spike stable equilibrium solution  $a$  (solid curve) and  $h$  (dotted curve) for the model in (2.33), with delay in both the activator regulation and inhibitor production. Right: Plot of the trajectory  $x_0(t)$  for the center of the spike. The dotted curve is the full numerical simulation obtained from (2.33), and the solid curve is the asymptotic result as obtained from (2.38), with delay in the  $h$  term of the activator equation. Parameter values used are  $T = 0.1$ ,  $\epsilon = 0.06$ ,  $\mu = 1$ , and  $D = 1$ .

## 2.4 Delay in the Activator Regulation and Catylyzation

In this subsection, we analyze the more difficult problem where the nonlinear term of the activator equation is delayed. The PDEs for this model are given by

$$a_t = \epsilon^2 a_{xx} - a + \frac{a_T^2}{h_T}, \quad 0 < x < L, t > 0 \quad (2.39a)$$

$$0 = Dh_{xx} - \mu h + \frac{a^2}{\epsilon}, \quad 0 < x < L, t > 0 \quad (2.39b)$$

with the same boundary conditions and assumptions as the model in (2.1).

Placing the delay in the non-linear term of the activator equation changes the dynamics of the system and makes it quite difficult to analyze. To simplify the analysis, we assume localized activator concentrations.

In the inner region, we let  $x_0(\tau)$  be the center of the spike, where  $\tau = \epsilon^2 t$ . In terms of the inner coordinate  $y$  and the inner variables  $A(y)$  and  $H(y)$ , as defined in (2.2) and (2.3), respectively, we can rewrite (2.39) as

$$-\epsilon A_y \dot{x}_0 = A_{yy} - A + \frac{A_T^2}{H_T}, \quad -\infty < y < \infty, \quad (2.40a)$$

$$0 = \frac{D}{\epsilon^2} H_{yy} - H + \frac{A^2}{\epsilon}, \quad -\infty < y < \infty. \quad (2.40b)$$

By definition, we have that

$$A_T = A\left(\frac{x - x_0(\tau - T)}{\epsilon}\right) = A\left(\frac{x - x_0(\epsilon^2 t - T)}{\epsilon}\right). \quad (2.41)$$

Using the expansion

$$x_0(\epsilon^2 t - T) \approx x_0(\epsilon^2 t) - \epsilon^2 T x'_0 + \dots = x_0(\tau) - \epsilon^2 T \dot{x}_0 + \dots, \quad (2.42)$$

we rewrite (2.41) as

$$A_T \approx A\left(\frac{x - x_0(\tau) + \epsilon^2 T \dot{x}_0}{\epsilon}\right) = A(y + \epsilon T \dot{x}_0). \quad (2.43)$$

Moreover, expanding the right hand side of (2.43) gives

$$A_T \approx A(y) + \epsilon T \dot{x}_0 A_y. \quad (2.44)$$

Using the inner variable expansion  $A(y) = A_0(y) + \epsilon A_1(y) + \dots$  and  $H(y) = H_0(y) + \epsilon H_1(y) + \dots$ , and the approximations  $A_{0T} \approx A_0 + \epsilon T \dot{x}_0 A_{0y}$ , and  $A_{1T} \approx A_1 + \epsilon T \dot{x}_0 A_{1y}$ , we get to leading order that equation (2.40a) becomes

$$\begin{aligned} -\epsilon A_{0y} \dot{x}_0 &= A_{0yy} - A_0 + \frac{A_0^2}{H_{0T}} \\ &+ \epsilon \left[ A_{1yy} - A_1 + 2 \frac{A_0}{H_{0T}} A_1 - \frac{A_0^2}{H_{0T}^2} H_{1T} + 2T \frac{A_0}{H_{0T}} A_{0y} \dot{x}_0 \right] + O(\epsilon^2). \end{aligned} \quad (2.45)$$

This implies that

$$0 = A_{0yy} - A_0 + \frac{A_0^2}{H_{0T}}, \quad \text{and} \quad (2.46a)$$

$$-A_{0y} \dot{x}_0 \left(1 + 2T \frac{A_0}{H_{0T}}\right) = A_{1yy} - A_1 + 2 \frac{A_0}{H_{0T}} A_1 - \left(\frac{A_0}{H_{0T}}\right)^2 H_{1T}. \quad (2.46b)$$

Therefore, the  $O(1)$  equations for the model in (2.39) are

$$0 = A_{0yy} - A_0 + \frac{A_0^2}{H_{0T}}, \quad -\infty < y < \infty, \quad (2.47a)$$

$$0 = D H_{0yy} \implies H(y) \approx H_0 = \text{constant}, \quad -\infty < y < \infty. \quad (2.47b)$$

Rescaling  $A_0$  in (2.47a) using  $A_0 = H_{0T} w(y)$ , yields the system in (2.6), with the unique solution  $w(y)$  in (2.7). For the next order expansion in (2.46b), we introduce the operator  $L(A_1)$  such that

$$L(A_1) \equiv A_{1yy} - A_1 + 2 \frac{A_0}{H_{0T}} A_1 = \left(\frac{A_0}{H_{0T}}\right)^2 H_{1T} - A_{0y} \dot{x}_0 \left(1 + 2T \frac{A_0}{H_{0T}}\right). \quad (2.48)$$

Using the rescaling  $A_0 = H_{0T} w(y)$ , (2.48) becomes

$$L(A_1) \equiv A_{1yy} - A_1 + 2w A_1 = \left(\frac{A_0}{H_{0T}}\right)^2 H_{1T} - \dot{x}_0 (A_{0y} + 2T A_{0y} w) \quad (2.49)$$

As before, we have that  $L(A_1) \equiv A_{1yy} - A_1 + 2wA_1$  must be orthogonal to the homogeneous solution  $w'$ . Therefore using this solvability condition, we multiply both sides of (2.49) by  $A_{0y}$  and integrating by parts twice to get

$$-\dot{x}_0 \left( \int A_{0y}^2 dy + 2TH_{0T} \int A_{0y} w w' dy \right) = \frac{1}{3H_{0T}^2} \left( \int A_0^3 dy \right) (H_{1yT}(\infty) + H_{1yT}(-\infty)), \quad (2.50)$$

where we again use the even property of  $H_{1yy}$ .

In the outer region, in terms of the Green's function (2.15), we have that  $H_{0T}$  satisfies (2.29). Substituting this solution into (2.50) and simplifying gives

$$\dot{x}_0 = - \left( \frac{7}{7 + 12T} \right) \frac{G_{x_T}^- + G_{x_T}^+}{G(x_{0T}; x_{0T})}, \quad (2.51)$$

where  $G_{x_T}^-$  and  $G_{x_T}^+$  are as defined in (2.31). In terms of the initial time scale we get the following asymptotic ODE for the motion of the spike:

$$\dot{x}_0 = -\epsilon^2 \left( \frac{7}{7 + 12T} \right) \left( \frac{\sinh(2x_{0T} - L)}{\cosh(x_{0T} - L) \cosh(x_{0T})} \right). \quad (2.52)$$

In figure 4 we compare this asymptotic result with the numerics for the full system in (2.39). We also give numerical examples to show that the equilibrium solution is stable for all values of the delay  $T$ , and therefore no Hopf bifurcation is observed in the position of the spike.

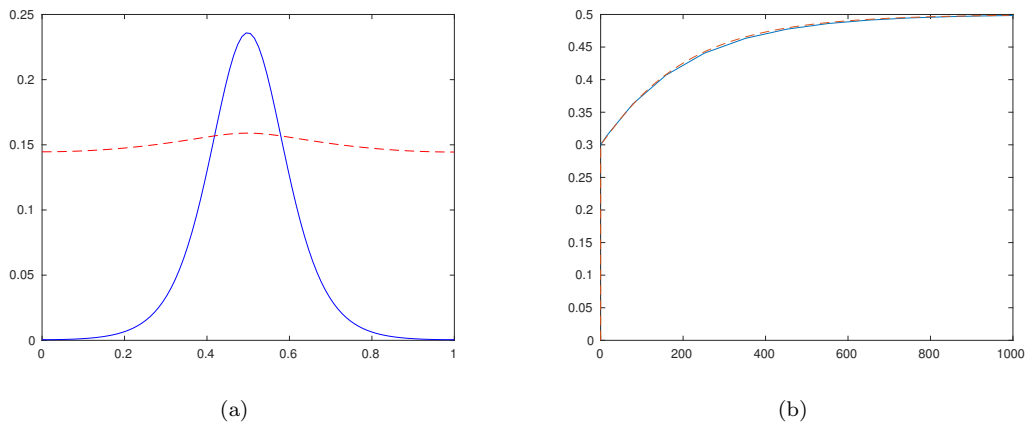


Figure 4: Left: Plot of the one-spike stable equilibrium solution  $a$  (solid curve) and  $h$  (dotted curve) for the model in (2.39), where the nonlinear term of the activator equation is delayed. Right: Plot of the trajectory  $x_0(t)$  for the center of the spike. The dotted curve is the full numerical simulation obtained from (2.39), and the solid curve is the asymptotic result as obtained from (2.52). Parameter values used are  $T = 0.1$ ,  $\epsilon = 0.06$ ,  $\mu = 1$ ,  $L = 1$  and  $D = 1$ .

## 2.5 Delay in All Non-Linear Terms in Both Equations

We now use the analysis and results in §2.3 and §2.4 to derive the differential equation corresponding to the following model where the non-linear terms of both equations are delayed:

$$a_t = \epsilon^2 a_{xx} - a + \frac{a_T^2}{h_T}, \quad 0 < x < L, t > 0, \quad (2.53a)$$

$$0 = Dh_{xx} - \mu h + \frac{a_T^2}{\epsilon}, \quad 0 < x < L, t > 0, \quad (2.53b)$$

$$a_x(0, t) = a_x(L, t) = h_x(0, t) = h_x(L, t) = 0. \quad (2.53c)$$

The ODE for the motion of the spike corresponding to the system in (2.53) is

$$\dot{x}_0 = -\epsilon^2 \left( \frac{7}{7 + 12T} \right) \left( \frac{\sinh(x_{0T} + x_{0T_2} - L)}{\cosh(x_{0T} - L) \cosh(x_{0T_2})} \right), \quad \text{where } T_2 = 2T. \quad (2.54)$$

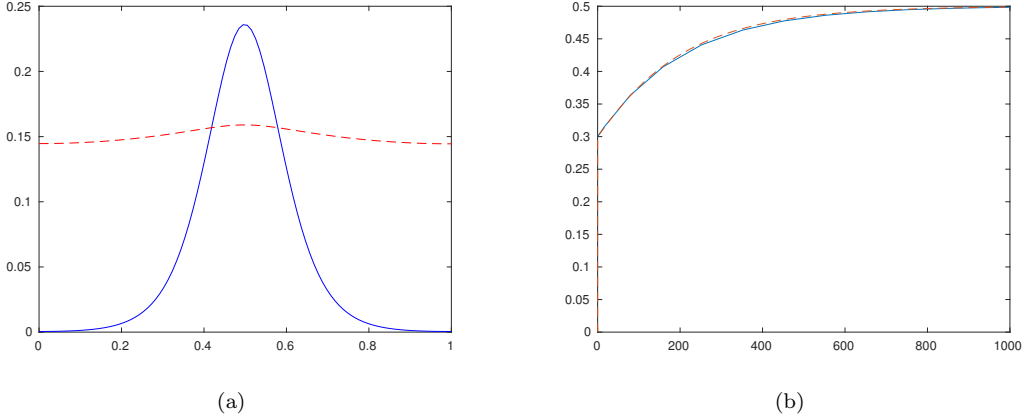


Figure 5: Left: Plot of the one-spike stable equilibrium solution  $a$  (solid curve) and  $h$  (dotted curve) for the model in (2.53), where all the nonlinear terms are delayed. Right: Plot of the trajectory  $x_0(t)$  for the center of the spike. The dotted curve is the full numerical simulation obtained from (2.53), and the solid curve is the asymptotic result as obtained from (2.54). Parameter values used are  $T = 0.1$ ,  $\epsilon = 0.06$ ,  $\mu = 1$ ,  $L = 1$  and  $D = 1$ .

## 3 Hopf Bifurcation in the Reduced Spike Location Equation

In this section, we consider how increasing the delay can bring about oscillations in the spike position. It is also possible for the large eigenvalues to undergo a Hopf bifurcation resulting in oscillation of the spike amplitudes. This will be considered in §4. For the delay models in §2, the spikes evolve on a slow  $O(\epsilon^2)$  time scale. We consider here the slowly moving spike as a quasi-equilibrium solution and analyze its stability by determining critical delay values at which a Hopf bifurcation occurs. The scaling of the critical delay for this Hopf bifurcation will thus be  $O(\epsilon^{-2})$ .

The critical delay for Hopf bifurcation consider in §4 will be scale as  $O(1)$  in  $\epsilon$ , so in general a Hopf bifurcation of the large eigenvalues will occur for smaller critical delay then that of the small eigenvalue.

In §2, we derived asymptotic delay differential equations of the form

$$\frac{dx_0}{dt} = f(x_{0T}, x_0), \quad 0 < x < L, t > 0. \quad (3.1)$$

We introduce a small perturbation to the equilibrium position

$$x_0(t) = x_0 + e^{\lambda t} \eta, \quad \text{where } |\eta| \ll |x_0|, \quad (3.2)$$

and we substitute (3.2) into (3.1) to get the following non-linear transcendental eigenvalue equation for  $\lambda$ :

$$\frac{dx_0}{dt} + \lambda e^{\lambda t} \eta = f(x_{0T}, x_0) + f_{x_{0T}}(x_{0T}, x_0) e^{\lambda(t-T)} \eta + f_{x_0}(x_{0T}, x_0) e^{\lambda t} \eta. \quad (3.3)$$

Since  $x_0$  is a solution of (3.1), therefore (3.3) simplifies to

$$\lambda = f_{x_{0T}}(x_{0T}, x_0) e^{-\lambda T} + f_{x_0}(x_{0T}, x_0). \quad (3.4)$$

Our goal is to solve (3.4) for critical values of the delay  $T$  which give rise to pure imaginary eigenvalues. Setting  $\lambda = i\omega$ , for  $\omega \in \mathbb{R}$ , in (3.4), and rearranging gives

$$\cos(\omega T) - i \sin(\omega T) = P(\omega, T) - i Q(\omega, T), \quad (3.5)$$

where the expressions  $P$  and  $Q$  are defined by

$$P(\omega, T) = -f_{x_0}/f_{x_{0T}}; \quad Q(\omega, T) = -\omega/f_{x_{0T}}. \quad (3.6)$$

Thus, from (3.5), we have that  $P$  and  $Q$  must satisfy the following system of equations:

$$P^2(\omega, T) + Q^2(\omega, T) = 1, \quad (3.7a)$$

$$\tan(\omega T) = \frac{Q(\omega, T)}{P(\omega, T)}. \quad (3.7b)$$

Without loss of generality, we now look for a positive solution  $(\omega_H, T_H)$  satisfying the equations in (3.7).

First, we consider the right hand side of (2.21),

$$f(x_{0T}, x_0) = -\epsilon^2 \left( \frac{\cosh(x_{0T} - L) \sinh(x_0) + \cosh(x_{0T}) \sinh(x_0 - L)}{\cosh(x_0 - L) \cosh(x_{0T})} \right), \quad (3.8)$$

with partial derivatives

$$f_{x_{0T}} = -\frac{\epsilon^2}{\cosh^2(x_{0T})}, \quad \text{and} \quad f_{x_0} = -\frac{\epsilon^2}{\cosh^2(x_0 - L)}. \quad (3.9)$$

Substituting (3.9) into (3.7a) yields

$$\frac{\epsilon^4}{\cosh^4(x_0 - L)} + \omega^2 = -\frac{\epsilon^2}{\cosh^2(x_{0T})}, \quad (3.10)$$

which has no positive real solution  $\omega$ , and therefore we conclude that no Hopf bifurcation occurs. This result is supported by numerical simulations for the full PDE model in (2.1) and the asymptotic result obtained from (2.21) for the position of the spike. In figure 1(a), we plot the equilibrium solution to (2.1). Spike position  $x_0 = 0.5L$  is stable, and that the slow moving spike tends towards this stable equilibrium for any choice of  $T$ , as shown in figure 6.

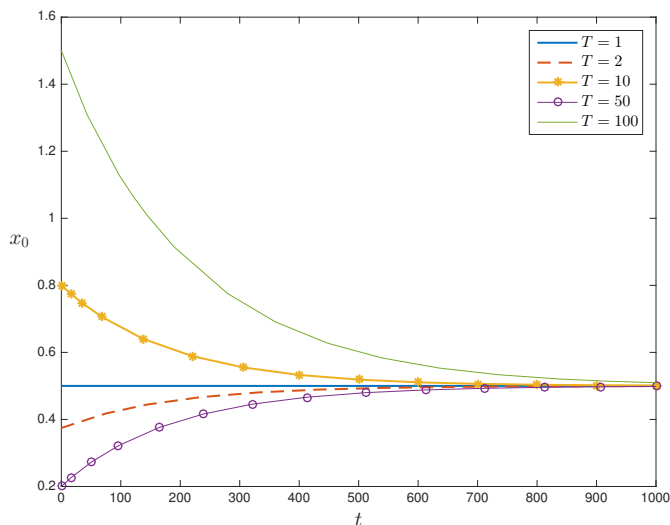


Figure 6: Plot of the motion of the center of the spike as obtained from the asymptotic ODE (2.21), with delay in the inhibitor equation. Increasing values of the delay  $T$  were used, and initial points as indicated. There are no oscillations in this case, and the equilibrium position  $x_0 = 0.5$  is always stable. Parameters used are  $\epsilon = 0.06$ ,  $\mu = 1$ , and  $D = 1$ .

For the result in (2.32), where delay appears in every term of the ODE, the asymptotic ODE is validated when compared to the full numerical simulation for (2.22). Moreover, we have that

$$f(x_{0T}, x_0) = -\epsilon^2 \left( \frac{\sinh(2x_{0T} - L)}{\cosh(x_{0T} - L) \cosh(x_{0T})} \right), \text{ and} \quad (3.11a)$$

$$f_{x_{0T}} = -\epsilon^2 \left( \frac{2 \cosh(2x_{0T} - L) \cosh(x_{0T} - L) \cosh(x_{0T}) - \sinh^2(2x_{0T} - L)}{\cosh^2(x_{0T} - L) \cosh^2(x_{0T})} \right). \quad (3.11b)$$

From (3.4), we get that

$$\lambda = f_{x_{0T}}(x_{0T}, x_0) e^{-\lambda T}. \quad (3.12)$$

Substituting  $\lambda = i\omega$  into (3.12), and comparing the real and imaginary parts on both sides of the equation gives

$$i\omega = \frac{\partial f}{\partial x_{0T}} e^{-i\omega T} \implies \begin{cases} f_{x_{0T}} \cos(\omega T) = 0, \text{ and} \\ -f_{x_{0T}} \sin(\omega T) = \omega. \end{cases} \quad (3.13)$$

Using Newton's method to solve the system in (3.13). The results are given in figure (7). For  $L = 2$  we find that  $T_h \sim 1.87$  and  $\omega_h \sim 0.84$ . In figure (8) we plot simulations of (2.32) for  $T$  above and below this value.

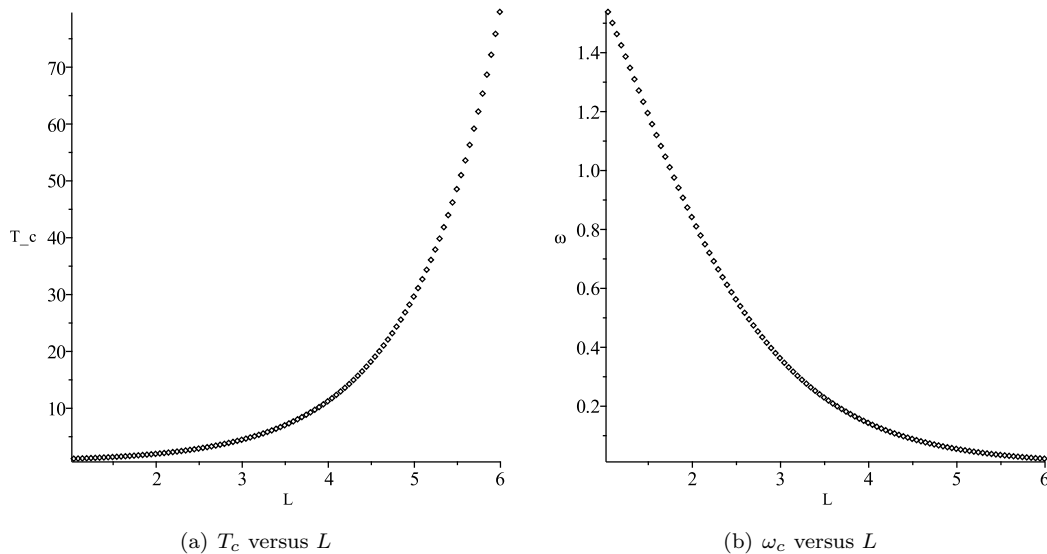


Figure 7: Solutions of (3.13) for various values of  $L$

Numerical simulations validate these results, and we find that for delay  $T < T_H$  the real part of  $\lambda$  is negative which gives rise to decaying oscillations that approach the stable equilibrium  $x_0 = \frac{L}{2}$ . However, for  $T > T_H$ , the equilibrium solution is unstable since the eigenvalue crosses the imaginary axis and the real part of  $\lambda$  becomes positive giving rise to sustained oscillations. These results are illustrated in figure 8.

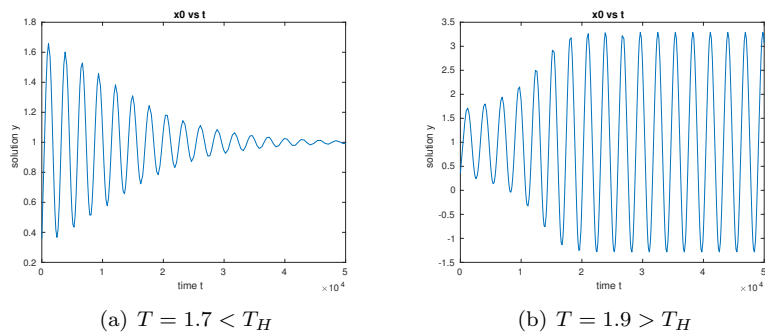


Figure 8: Plot of the asymptotic result  $x_0(t)$  as obtained from (2.32), with delay in the  $h$  term of the activator equation, for delay  $T = 1.7 < T_H$  (left figure) and  $T = 1.9 > T_H$  (right figure). Parameters used are  $\epsilon = 0.6$ ,  $\mu = 1$ ,  $L = 2$  and  $D = 1$ .

Next, we consider the asymptotic result in (2.38), where

$$\frac{dx_0}{dt} = f(x_{0T_1}, x_{0T_2}) = -\epsilon^2 \left( \frac{\sinh(x_{0T_1} + x_{0T_2} - L)}{\cosh(x_{0T_1} - L) \cosh(x_{0T_2})} \right), \quad \text{where } T_2 = 2T_1, \quad (3.14)$$

with partial derivatives

$$f_{x_{0T_1}} = -\epsilon^2 \left( \frac{1}{\cosh^2(x_{0T_1} - L)} \right); \quad f_{x_{0T_2}} = -\epsilon^2 \left( \frac{1}{\cosh^2(x_{0T_2})} \right). \quad (3.15)$$

Substituting the small perturbation (3.2) into (3.14) gives the transcendental eigenvalue equation

$$\lambda = f_{x_{0T_1}} e^{-\lambda T_1} + f_{x_{0T_2}} e^{-\lambda T_2}, \quad \text{where } T_2 = 2T_1. \quad (3.16)$$

Setting  $\lambda = i\omega$  in (3.16), and comparing the real and imaginary parts on both sides of the equation, gives that  $\omega$  and delays  $T_1$  and  $T_2$  must satisfy the following system of equations:

$$f_{x_{0T_1}} \cos(\omega T_1) + f_{x_{0T_2}} \cos(\omega T_2) = 0; \quad f_{x_{0T_1}} \sin(\omega T_1) + f_{x_{0T_2}} \sin(\omega T_2) = -\omega. \quad (3.17)$$

We again use Newton's method to solve (3.17). In figure 9 we plot the critical values of  $T$  and  $\omega$  for various values of  $L$ . For the case  $L = 3$ , we find  $T_H \sim 1.44$  and  $\omega_H \sim 0.727$ .

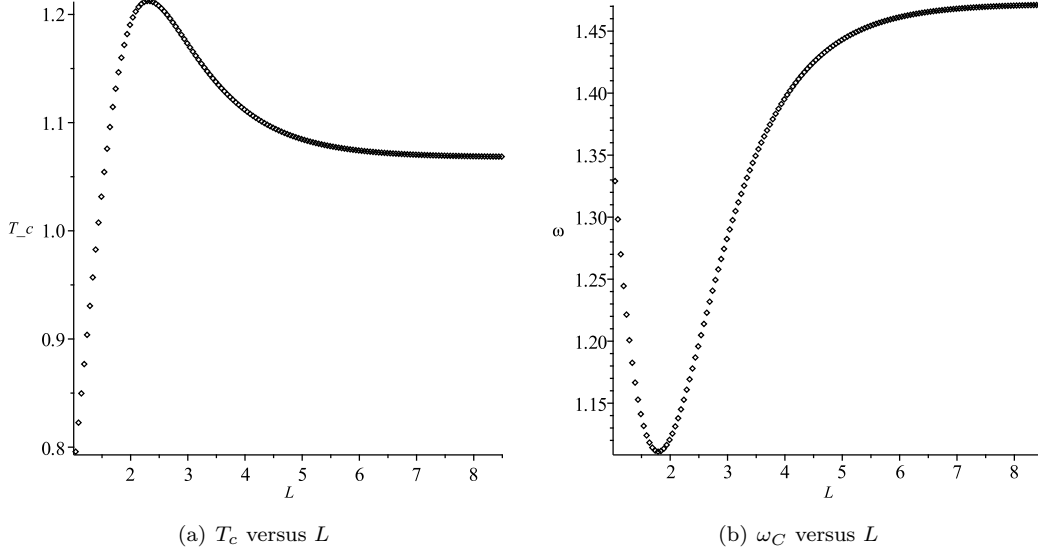


Figure 9: Solutions of (3.17) for a range of  $L$

$$(\omega_H, T_{1H}, T_{2H}) = (0.49, 2.14, 4.28). \quad (3.18)$$

The asymptotic ODE for this case is validated when compared to the full numerical simulation, as shown in figure 3. Moreover, as illustrated in figure 10, for delay less than the critical value

we have that the real part of the eigenvalue is negative and the decaying oscillations approach the stable equilibrium position  $x_0 = 0.5$ . However, as we increase the delay beyond the Hopf value, the equilibrium solution is destabilized as the eigenvalue crosses the imaginary axis resulting in sustained oscillations.

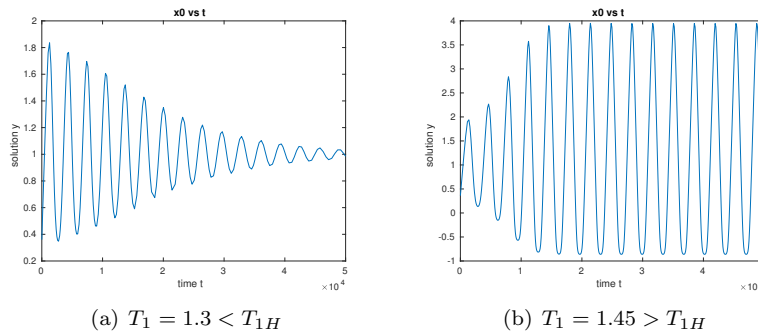


Figure 10: Plot of the asymptotic result  $x_0(t)$  as obtained from (2.38), where delay is in both the activator and inhibitor equations, for delay values  $T_1 = 1.3$  (left figure) and  $T_1 = 1.45$  (right figure). Parameters used are  $\epsilon = 0.6$ ,  $\mu = 1$ ,  $L = 2$  and  $D = 1$ .

Similarly, the result in (2.52) gives that

$$f(x_{0T}, x_0) = -\epsilon^2 \left( \frac{7}{7 + 12T} \right) \left( \frac{\sinh(2x_{0T} - 1)}{\cosh(x_{0T} - 1) \cosh(x_{0T})} \right); \quad (3.19a)$$

$$f_{x_{0T}} = -\epsilon^2 \left( \frac{7}{7 + 12T} \right) \left( \frac{2 \cosh(2x_{0T} - 1) \cosh(x_{0T} - 1) \cosh(x_{0T}) - \sinh^2(2x_{0T} - 1)}{\cosh^2(x_{0T} - 1) \cosh^2(x_{0T})} \right), \quad (3.19b)$$

where  $f_{x_{0T}}$  satisfies (3.13). Upon substituting the expressions in (3.19) into (3.13), we find that a positive solution  $(\omega, T)$  exists such that the two equations in (3.13) are both satisfied only if  $\epsilon > 1$ , which is a contradiction to our initial assumption. Thus, in this case the equilibrium solution is stable for all positive values of  $T$ . In figure 4, we compare the asymptotic ODE with the full numerical simulation, and in figure 11 the results above are validated with numerical simulations, where we plot various trajectories of the asymptotic solution  $x_0(t)$  for increasing values of delay as they approach the stable equilibrium position  $x_0 = 0.5$ .

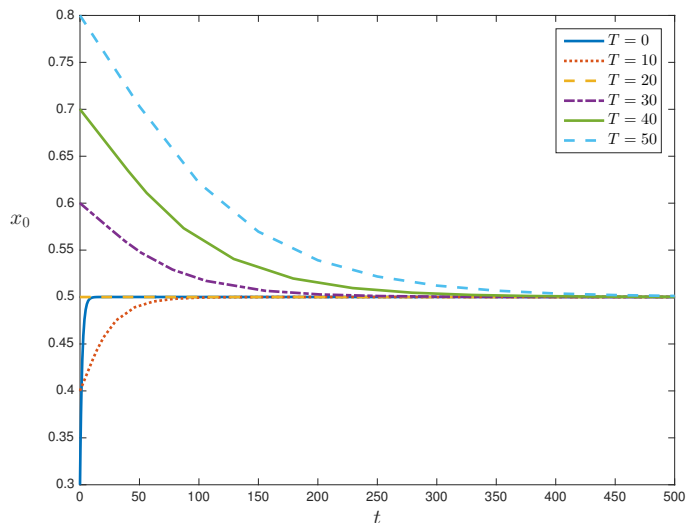


Figure 11: Plot of trajectories corresponding to motion of the spike as obtained from the asymptotic ODE (2.52), with increasing values of delay in the non-linear term of the activator equation, and using various initial points as indicated. No oscillations are observed and all trajectories approach the stable equilibrium position  $x_0 = 0.5$ . Parameters used are  $\epsilon = 0.6$ ,  $\mu = 1$ , and  $D = 1$ .

A similar outcome to the illustrated in figure 11 is obtained when the full PDE model (2.53) and the asymptotic ODE (2.54) are numerically analyzed. As in the previous case, for  $\epsilon < 1$ , there is no positive solution  $(\omega, T)$  such that (3.13) is satisfied, and all trajectories  $x_0(t)$  approach the stable equilibrium  $x_0 = 0.5$  for all values of the delay  $T$ .

## 4 Stability Analysis for the Spike Profile: Derivation of Non-local Eigenvalue Problem

In this section, we consider the delayed Gierer-Meinhardt models in §2, and we study oscillatory-type instabilities in the height of the one-spike solution for each model. This analysis is an extension of the work done in [19] with no delay. We begin by formulating the nonlocal eigenvalue problem (NLEP) in each case, and we find conditions for the onset of a Hopf bifurcation. The results are then compared with the numerics obtained from the full system.

For the model in (2.1), with delay in the inhibitor equation, we assume  $0 < \sigma \ll 1$  and  $D = O(1)$ . To simplify the notation, we let  $\mu = 1$ ,  $D = 1$  and let the length of the domain,  $L$ , vary. By symmetry, the spike location is  $x_0 = L/2$ , and as before we use the time scaling  $\tau = \epsilon^2 t$ . Using the notation in [19], as  $\epsilon \rightarrow 0$ , the equilibrium solutions are given by

$$a_e(x) \sim H w \left[ \frac{x - x_0(\tau)}{\epsilon} \right]; \quad h_e(x) \sim \frac{H}{a_g} G(x; x_0), \quad \text{for } 0 < x < L, \quad (4.1)$$

where  $w$  is the unique solution (2.7) and the Green's function  $G(x; x_0)$  satisfies (2.14). Here the

constants  $H$  and  $a_g$ , for which  $h_e(x) = H$ , are defined by

$$H = \frac{1}{b a_g}; \quad b = \int_{-\infty}^{\infty} [w(y)]^2 dy = 6; \quad a_g = \cosh^2(L/2) / \sinh(L/2). \quad (4.2)$$

To analyze the stability of the equilibrium solutions (4.1), we introduce the small perturbations

$$a(x, t) = a_e(x) + e^{\lambda t} \phi(x); \quad h(x, t) = h_e(x) + e^{\lambda t} \eta(x), \quad \text{where } \phi, \eta \ll 1. \quad (4.3)$$

Substituting (4.3) into the original PDE model (2.1) gives the following eigenvalue problem:

$$\lambda \phi = \epsilon^2 \phi_{xx} - \phi + 2 \frac{a_e}{h_e} \phi - \frac{a_e^2}{h_e^2} \eta, \quad 0 < x < L, \quad (4.4a)$$

$$D \eta_{xx} - (1 + \sigma \lambda) \eta = -2 \frac{a_e}{\epsilon} e^{-\lambda T} \phi, \quad 0 < x < L, \quad (4.4b)$$

with the Neumann boundary conditions

$$\phi_x(0) = \phi_x(L) = \eta_x(0) = \eta_x(L) = 0. \quad (4.5)$$

We now introduce the new variables

$$a_e = H u; \quad \phi = H \bar{\phi}; \quad h_e = H v; \quad \eta = H \bar{\eta}. \quad (4.6)$$

Substituting these new variables into (4.4), and dropping the bar notation, yields the eigenvalue problem

$$\lambda \phi = \epsilon^2 \phi_{xx} - \phi + 2 \frac{u}{v} \phi - \frac{u^2}{v^2} \eta, \quad 0 < x < L, \quad (4.7a)$$

$$D \eta_{xx} - (1 + \sigma \lambda) \eta = -2 \frac{u}{\epsilon b a_g} e^{-\lambda T} \phi, \quad 0 < x < L, \quad (4.7b)$$

with boundary conditions (4.5). The constants  $b$  and  $a_g$  are as defined in (4.2).

As in [19], we look for a localized eigenfunction  $\phi$  of the form

$$\phi(x) \sim C_0 \Phi \left( \frac{x - x_0}{\epsilon} \right). \quad (4.8)$$

Near  $x = x_0$  the eigenfunction  $\phi$  is localized, and we can treat the right-hand side expression in (4.7b) as a multiple of the Dirac delta function. Thus, for  $\epsilon \ll 1$ , we get that  $\eta$  satisfies

$$D \eta_{xx} - (1 + \sigma \lambda) \eta = -\frac{2}{a_g} e^{-\lambda T} \left( \frac{\int_{-\infty}^{\infty} w \Phi(y) dy}{\int_{-\infty}^{\infty} w^2 dy} \right) C_0 \delta(x - x_0), \quad 0 < x < L, \quad (4.9a)$$

$$\eta_x(0) = \eta_x(L) = 0, \quad (4.9b)$$

for  $0 < x < 1$ . Following the same process as in [19], while accounting for the effect of delay, yields the following nonlocal eigenvalue problem for  $\Phi(y)$ :

$$L_0 \Phi - \chi(\lambda) w^2 \left( \frac{\int_{-\infty}^{\infty} w \Phi(y) dy}{\int_{-\infty}^{\infty} w^2 dy} \right) = \lambda \Phi, \quad -\infty < y < \infty, \quad (4.10a)$$

$$\Phi(0) \rightarrow 0 \quad \text{as} \quad |y| \rightarrow \infty, \quad (4.10b)$$

where the linear operator  $L_0$  and  $\chi(\lambda)$  are given by

$$L_0\Phi \equiv \Phi'' - \Phi + 2w\Phi; \quad \chi(\lambda) = \frac{2e^{-\lambda T}}{a_g \sqrt{(1 + \sigma\lambda)D}}. \quad (4.11)$$

As shown in [5] and [19], any unstable eigenvalue of (4.10) must be a root of  $g(\lambda) = 0$ , where

$$g(\lambda) = C(\lambda) - f(\lambda); \quad C(\lambda) = \frac{1}{\chi(\lambda)}; \quad f(\lambda) = \frac{\int_{-\infty}^{\infty} w [L_0 - \lambda]^{-1} w^2 dy}{\int_{-\infty}^{\infty} w^2 dy}. \quad (4.12)$$

To determine the smallest positive delay value at which a Hopf bifurcation occurs, we seek pure imaginary eigenvalues, along the positive imaginary axis, that satisfy (4.12). Setting  $\lambda = i\lambda_I$  in (4.12) and separating the real and imaginary components gives the coupled system

$$g_R(\lambda_I) = g_I(\lambda_I) = 0, \quad (4.13)$$

where,

$$g_R(\lambda_I) = C_R(\lambda_I) - f_R(\lambda_I); \quad g_I(\lambda_I) = C_I(\lambda_I) - f_I(\lambda_I); \quad (4.14a)$$

$$C_R(\lambda_I) = \text{Re}[C(i\lambda_I)]; \quad C_I(\lambda_I) = \text{Im}[C(i\lambda_I)]; \quad (4.14b)$$

$$f_R(\lambda_I) = \frac{\int_{-\infty}^{\infty} w L_0 [L_0^2 + \lambda_I^2]^{-1} w^2 dy}{\int_{-\infty}^{\infty} w^2 dy}; \quad f_I(\lambda_I) = \frac{\lambda_I \int_{-\infty}^{\infty} w [L_0^2 + \lambda_I^2]^{-1} w^2 dy}{\int_{-\infty}^{\infty} w^2 dy}. \quad (4.14c)$$

To simplify the notation, we let  $\sigma = 0$  and  $D = 1$ , which gives  $a_g = \cosh^2(L/2)/\sinh(L)$ . Thus, we have

$$C_R(\lambda_I) = \frac{\cosh^2(L/2)}{2\sinh(L)} \cos(\lambda_I T); \quad C_I(\lambda_I) = \frac{\cosh^2(L/2)}{2\sinh(L)} \sin(\lambda_I T). \quad (4.15)$$

Approximating the solution to (4.15) using an iterative method, we plot the critical values of  $T$  and  $\omega$  in figure 12. For  $L = 1$  we find that a Hopf bifurcation occurs at the critical parameter values

$$(\lambda_{IH}, T_H) = (1.827450252, 0.5193320362). \quad (4.16)$$

In figure 13, we plot simulations of (2.1) for  $T$  above and below the critical value.

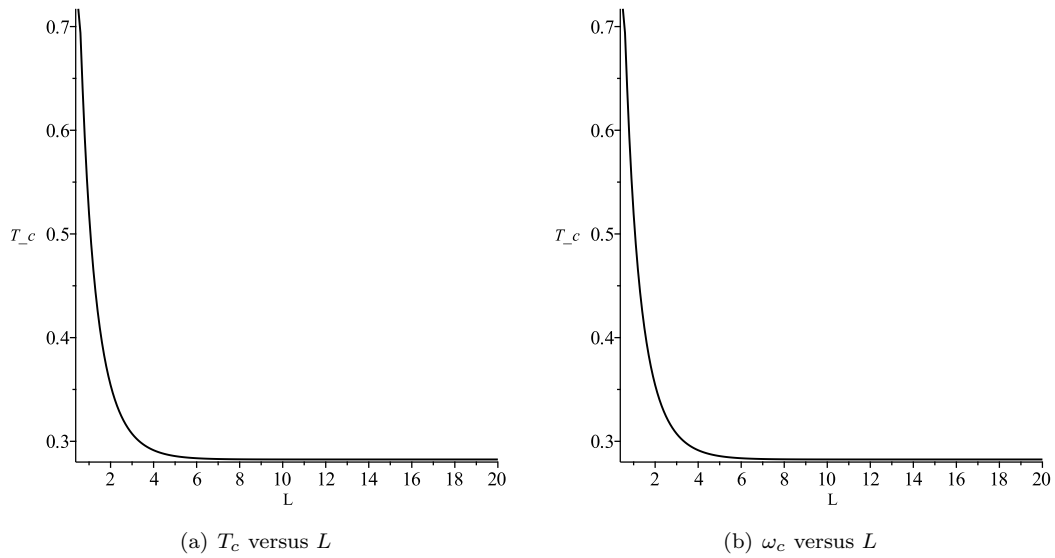


Figure 12: Solution to (4.15) for various values of  $L$

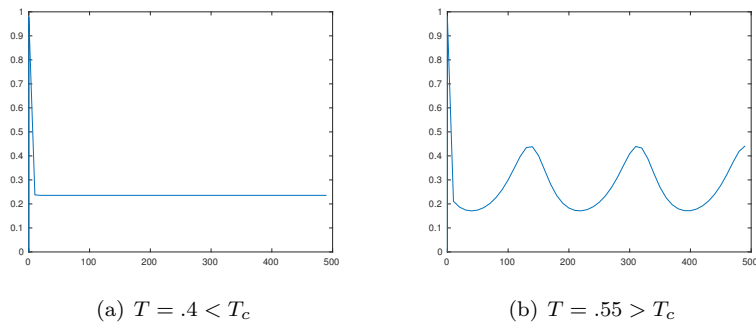


Figure 13: Amplitude of spike solution to (2.1) for delay below and above the critical value of  $T_c = 0.519$ . Here  $D = 1$ ,  $\mu = 1$ ,  $L = 1$  and  $\epsilon = 0.06$ .

The model in (2.22), with delay in the  $h$  term of the activator equation, yields the nonlocal eigenvalue problem in (4.10), where  $\chi(\lambda)$  is defined by (4.11). Thus, the results for this case are identical to the one delay case considered above.

Next we consider the model in (2.33) where delay is in both equations. The eigenvalue problem

for this case is given by

$$\lambda\phi = \epsilon^2\phi_{xx} - \phi + 2\frac{a_e}{h_e}\phi - \frac{a_e^2}{h_e^2}e^{-\lambda T}\eta, \quad 0 < x < L, t > 0, \quad (4.17a)$$

$$D\eta_{xx} - (1 + \sigma\lambda)\eta = -2\frac{a_e}{\epsilon}e^{-\lambda T}\phi, \quad 0 < x < L, t > 0, \quad (4.17b)$$

$$\phi_x(0) = \phi_x(L) = \eta_x(0) = \eta_x(L) = 0. \quad (4.17c)$$

Moreover, the corresponding nonlocal eigenvalue problem is

$$L_0\Phi - \chi(\lambda)w^2\left(\frac{\int_{-\infty}^{\infty}w\Phi(y)dy}{\int_{-\infty}^{\infty}w^2dy}\right) = \lambda\Phi, \quad -\infty < y < \infty, \quad (4.18)$$

$$\Phi(y) \rightarrow 0 \text{ as } |y| \rightarrow \infty, \quad (4.19)$$

where  $\chi$  is defined by

$$\chi(\lambda) = \frac{2e^{-2\lambda T}}{a_g\sqrt{(1 + \sigma\lambda)D}}. \quad (4.20)$$

The only difference is the delay is multiplied by two. Thus the critical value of delay should be half of that in the cases considered. In figure 14 we simulate system (2.33) above and below the critical values.

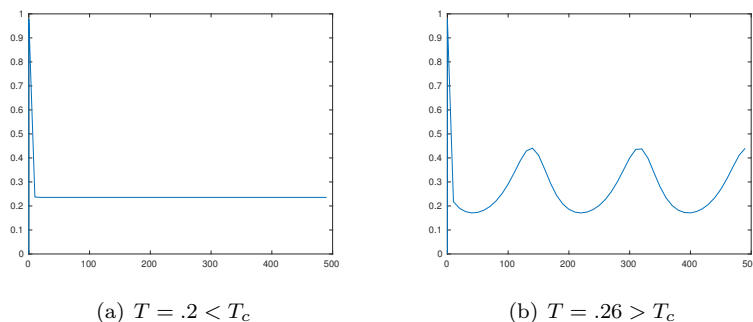


Figure 14: Amplitude of spike solution to (2.33) for delay below and above the critical value of  $T_c \sim 0.25$ . Here  $D = 1$ ,  $\mu = 1$ ,  $L = 1$  and  $\epsilon = 0.06$ .

We now consider the more difficult case in (2.39), where the nonlinear reaction term of the activator equation is delayed. The corresponding nonlocal eigenvalue problem for  $\Phi(y)$  is given by

$$\Phi'' - \Phi + 2we^{-\lambda T}\Phi - \chi(\lambda)w^2\left(\frac{\int_{-\infty}^{\infty}w\Phi(y)dy}{\int_{-\infty}^{\infty}w^2dy}\right) = \lambda\Phi, \quad -\infty < y < \infty, \quad (4.21a)$$

$$\Phi(y) \rightarrow 0 \text{ as } |y| \rightarrow \infty, \quad (4.21b)$$

where  $\chi(\lambda)$  is defined by

$$\chi(\lambda) = \frac{2e^{-\lambda T}}{a_g\sqrt{(1 + \sigma\lambda)D}}. \quad (4.22)$$

Due to the presence of the right hand side term  $2we^{-\lambda T}\Phi$ , we are not able to utilize the methods used earlier. Instead, a numerical method is used to approximate and analyze the corresponding large eigenvalues. Assuming  $\epsilon \ll 1$ , we split the right hand side of (4.21a) into two parts,

$$A\Phi \equiv \Phi'' - \Phi + 2we^{-\lambda T}\Phi; \quad \text{and} \quad B\Phi \equiv \chi(\lambda)w^2 \left( \frac{\int_{-\infty}^{\infty} w\Phi(y)dy}{\int_{-\infty}^{\infty} w^2 dy} \right), \quad (4.23)$$

and we introduce a new operator  $L_\delta\Phi$  defined by

$$L_\delta\Phi \equiv A\Phi - \delta B\Phi, \quad -\infty < y < \infty. \quad (4.24)$$

We note that for  $\delta = 0$  we get a Sturm-Liouville equation similar to the ones analyzed above.

Next, we discretize the finite domain problem for  $\epsilon \ll 1$ . The operator  $L\delta$  can be approximated using a discrete linear operator, denoted by  $\mathcal{M}$ , using the centered difference approximation of the second derivative for the operator  $A\Phi$ , and the Trapezoidal rule approximation for  $B\Phi$ . Thus the corresponding eigenvalues can be approximated by the eigenvalues of the matrix  $\mathcal{M}$ , denoted by  $\lambda_i(\delta)$ .

In the absence of delay, we set  $T = 0$  and we use a continuation method where we start with an initial guess for  $\delta = 0$ , and we continue to track the principal eigenvalue of the matrix as  $\delta$  increases. As expected, we find that  $\lambda_0 \rightarrow 5/4$  as  $\delta \rightarrow 0$ , which is the eigenvalue corresponding to the eigenfunction  $\Phi_0 = \text{sech}^2(y/2)$ . Furthermore, as the value of  $\delta$  is increased, we find that  $\lambda_0 \approx 0$  for  $\delta = 1/2$ . Shortly after this point, the eigenvalues collide and eventually become complex with the real part of  $\lambda_0$  remaining negative as  $\delta \rightarrow 1$ .

Next, we introduce delay, and we use the method of successive substitution to track the eigenvalues. We continue with this iterative method until the difference between successive iterates is less than  $10^{-11}$ . This repeated as the delay value  $T$  increased from 0.005 to 2.2. The results are illustrated in figure 15, which shows that the real part of  $\lambda_0$  remains negative as  $T$  increases. Thus, in this case the solution is stable and no oscillations are observed. We repeated the process for different values of  $L$  and similar results are found in each case. In [6] it is found that this form of delay can actually aid in the stabilization of spike solutions. Simulations of (2.39) with delay values of up to 50 resulted in stable solutions with no oscillations.

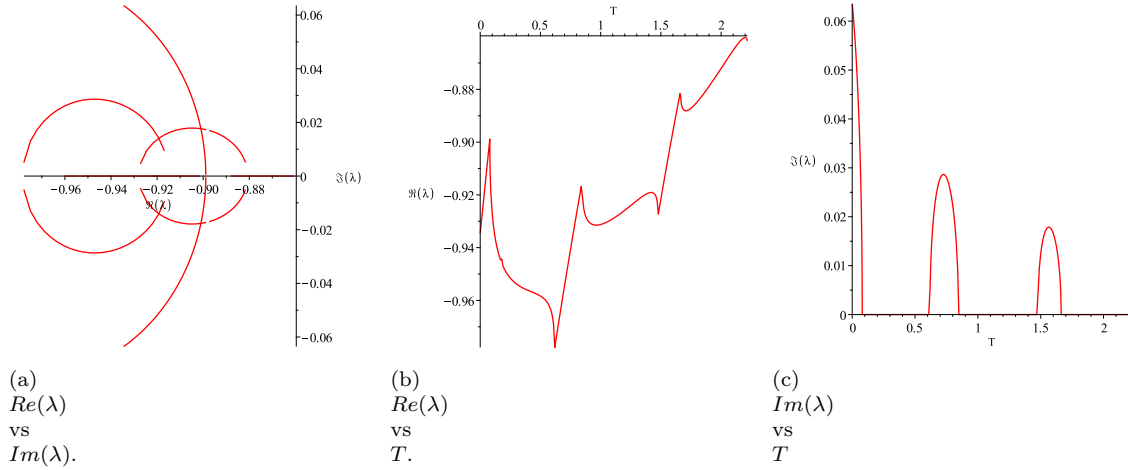


Figure 15: Plot of  $Re(\lambda_0)$  versus  $Im(\lambda_0)$  for the eigenvalue of matrix  $\mathcal{M}$ .

Finally, for the case in (2.53), where both nonlinear reaction terms are delayed, the corresponding nonlocal eigenvalue problem is

$$\Phi'' - \Phi + 2we^{-\lambda T}\Phi - \chi(\lambda)w^2 \left( \frac{\int_{-\infty}^{\infty} w\Phi(y)dy}{\int_{-\infty}^{\infty} w^2 dy} \right) = \lambda\Phi, \quad -\infty < y < \infty, \quad (4.25a)$$

$$\Phi(y) \rightarrow 0 \text{ as } |y| \rightarrow \infty, \quad (4.25b)$$

where  $\chi(\lambda)$  is given by

$$\chi = \frac{2e^{-2\lambda T}}{a_g \sqrt{(1 + \sigma\lambda)D}}. \quad (4.26)$$

The resulting system is very similar to the previous case. Again we find that no hopf bifurcations occur as the delay is increased and simulations of the system with delay values up to fifty show no signs of oscillation.

## 5 Oscillations in Spike Position

The critical value of delay causing oscillations in the spike position scales as  $O(\epsilon^{-2})$  as compared to  $O(1)$  in  $\epsilon$  for amplitude oscillations. For all the cases we have considered, amplitude oscillations are triggered well before the onset of oscillations in spike position. In this section, we will consider what can happen if we have delay in the degradation of activator,

$$a_t = \epsilon^2 a_{xx} - a_T + \frac{a^2}{h}, \quad 0 < x < L, t > 0, \quad (5.1a)$$

$$\sigma h_t = Dh_{xx} - \mu h + \frac{a^2}{\epsilon}, \quad 0 < x < L, t > 0. \quad (5.1b)$$

We cannot justify this case biologically, however this is the only case we have found in which spike positional oscillations for the Gierer-Meinhardt system can occur and the behaviour is worthy of

study. It is fairly simple see how oscillations arise in this case. If we derive the eigenvalue problem in the usual way, we find

$$\lambda\phi = \epsilon^2\phi_{xx} - e^{-\lambda T}\phi + 2\frac{a_e}{h_e}\phi - \frac{a_e^2}{h_e^2}\eta, \quad 0 < x < L, \quad (5.2a)$$

$$D\eta_{xx} - (1 + \sigma\lambda)\eta = -2\frac{a_e}{\epsilon}\phi, \quad 0 < x < L, \quad (5.2b)$$

with the Neumann boundary conditions

$$\phi_x(0) = \phi_x(L) = \eta_x(0) = \eta_x(L) = 0. \quad (5.3)$$

Since the eigenvalues associated with the translation eigenfunctions are small, we set  $\lambda = \epsilon^2\lambda_0 + \dots$ , plug into our system and expand in a Taylor Series. The first equation then becomes

$$(\epsilon^2\lambda_0 + \dots)\phi = \epsilon^2\phi_{xx} - (1 - \epsilon^2\lambda_0 T + \dots)\phi + 2\frac{a_e}{h_e}\phi - \frac{a_e^2}{h_e^2}\eta,$$

or

$$(\epsilon^2\lambda_0(1 - T) + \dots)\phi = \epsilon^2\phi_{xx} - (1 + \dots)\phi + 2\frac{a_e}{h_e}\phi - \frac{a_e^2}{h_e^2}\eta.$$

The leading order term or the small eigenvalue is simply multiplied by  $(1 - T)$ . So, as  $T$  crosses 1, the small eigenvalue changes sign. In the simulations below, we find clear evidence of a Hopf bifurcation in the spike location as  $T$  increases past 1.

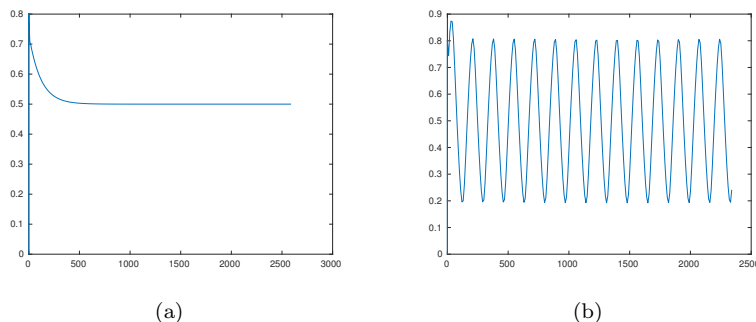


Figure 16: Simulations of (5.1) with  $D = 1$ ,  $\mu = 1$ ,  $L = 1$ . In 16(a),  $T = .9$  and in 16(b),  $T = 1.04$ .

To be complete, we would need to show that at  $T = 1$ , the eigenvalue associated with the spike amplitude is negative. However, such a calculation would require converting to a discrete operator and approximating the eigenvalue numerically. A numerical simulation of the partial differential equations such as that illustrated in figure 16(b) suggests such an eigenvalue is negative, at least in that particular case.

## 6 Discussion

In this paper, we have analyzed the stability of the slowly evolving spike solutions to the 1-dimensional GM model with delayed reaction-kinetics. Delay is a natural extension of the GM

model and is well motivated biologically due to time delays needed for protein synthesis and gene expression. Moreover, we have delayed various nonlinear terms in the model in order to mimic all the possible ways delay could show up in the reaction. The analysis and results given have been derived using asymptotic and numerical methods.

In §2, we have shown that the model PDE equations can be reduced to a system of delay ODEs representing the motion for the corresponding spike solution. In §2.3, although the original PDE has only one delay, the resulting reduced system has two different delays. In §2.4 and §2.5, the presence of delay in the activator catalysis term introduces some complications to the analysis. In all cases, simulations of the reduced system agree with simulations of the full partial differential equation.

In §3, we consider the Hopf bifurcation in the reduced system. Such a bifurcation would cause oscillation in the spike positions. In all cases where such a bifurcation is possible, the critical value of the delay is  $O\left(\frac{1}{\epsilon^2}\right)$  and a Hopf bifurcation causing a profile instability will have already occurred. In §4 we consider a Hopf bifurcation of the large eigenvalues. Such a bifurcation would result in oscillations of the spike amplitude. In this case the critical delay value is of  $O(1)$ . We find that increasing delay causes a Hopf bifurcation in all cases except for the systems (2.39) and (2.53). In these cases increasing delay does not cause a Hopf bifurcation in either the small or large eigenvalues. Simulations of the system of partial differential equations with large delay values verify the absence of a Hopf bifurcation. Simulations of the full system suggest that the Hopf bifurcations of the large eigenvalue are all sub-critical the resulting oscillations are unstable. Finally in §5, we consider a delay in activator degradation. Such a system is not biologically relevant, however, this is the only example of a Hopf bifurcation of the small eigenvalues for the Gierer-Meinhardt system. Simulations of the system suggest that this bifurcation is super-critical and the oscillations are sustained.

The study of delayed partial differential equations is a relatively new field and there are very few analytical results. The behaviour of systems with highly localized solutions can be analyzed by considering a much simpler system of ordinary differential equations. This reduction allows us to study the effect of delay on a system of partial differential equations. The methods considered in this paper can be applied to any reaction-diffusion system which supports highly localized solutions. We have only considered solutions with a spike type solution. Investigation into systems which support front type solutions could yield more interesting results. In addition, there is a great deal of work to be done in the area of numerical simulations of partial differential equations with delay.

## References

- [1] U. Ascher, S. J. Ruuth, R. J. Spiteri, *Implicit-explicit Runge-Kutta methods for time-dependent partial differential equations*, Applied Numerical Methods (1997) volume 25, issue 2-3, 151-167
- [2] S. Chen, J. Shi, *Global attractivity of equilibrium in Gierer-Meinhardt system with activator production saturation and gene expression time delays*, Nonlinear Analysis: Real World Applications 14(2013) 1871-1886
- [3] S. Chen, J. Shi, *Global attractivity of equilibrium in Gierer-Meinhardt system with activator production saturation and gene expression time delays*, Nonlinear Analysis: Real World Appl., 14(4), (2013), pp. 1871-1886.

- [4] X. Chen, M. Kowalczyk, *Dynamics of an interior spike in the Gierer-Meinhardt system*, SIAM J. Math. Anal., **33**, (2001), pp. 172-193.
- [5] N. Fadai, M. J. Ward, J. Wei, *The stability of spikes in the Gierer-Meinhardt model with delayed reaction-kinetics*, to be submitted, SIAM J. Appl. Math., (December 2015), (23 pages).
- [6] N. Fadai, M. Ward, J. Wei, *A Time-Delay in the Activator Kinetics Enhances the Stability of a Spike Solution to the Gierer-Meinhardt Model*, DCDS-B, accepted
- [7] A. Gierer, H. Meinhardt, *A theory of biological pattern formation*, Kybernetik, **12**, (1972), pp. 30-39.
- [8] D. Iron, C. Levy, *Dynamics and stability of a three-dimensional model of cell signal transduction with delay*, Nonlinearity, **28**(7), (2015), pp. 2515-2554.
- [9] D. Iron, M. J. Ward, *A metastable spike solution for a non-local reaction-diffusion model*, SIAM J. Appl. Math., **60**(3), (2000), pp.778-802.
- [10] D. Iron, M. J. Ward, *The dynamics of multispoke solutions to the one-dimensional Gierer-Meinhardt model*, SIAM J. Appl. Math., **62**(6), (2002), pp. 1924-1951.
- [11] D. Iron, M. J. Ward, J. Wei, *The stability of spike solutions to the one-dimensional Gierer-Meinhardt model*, Physica D, **150**(1-2), (2001), pp. 25-62.
- [12] S. Lee, E. A. Gaffney, N. A. M. Monk, *The influence of gene expression time delays on Gierer-Meinhardt pattern formation systems*, Bulletin of mathematical biology (2010) 72:2139-2160
- [13] S. Lee, E. A. Gaffney, N. A. M. Monk, *The influence of gene expression time delays on Gierer-Meinhardt pattern formation systems*, Bull. Math. Bio., **72**(8), (2010), pp. 2139-2160.
- [14] T. Kolokolnikov, J. Wei, *Stability of spike solutions in a competition model with cross-diffusion*, SIAM J. Appl. Math., **71**(4), (2011), pp. 1428-1457.
- [15] Y. Nec, M. J. Ward, *An explicitly solvable nonlocal eigenvalue problem and the stability of a spike for a sub-diffusive reaction-diffusion system*, Math. Model. of Nat. Phenom., **8**(2), (2013), pp. 55-87.
- [16] A. Turing, *The Chemical Basis of Morphogenesis*, Phil. Trans. Roy. Soc. B, **327**, (1952), pp. 37-72.
- [17] M. Van Dyke, *Perturbation methods in fluid mechanics*. Applied Mathematics and Mechanics, **8**, (1964).
- [18] M. J. Ward, J. Wei, *Hopf bifurcation of spike solutions for the shadow Gierer-Meinhardt model*, Europ. J. Appl. Math., **14**(6), (2003), pp. 667-711.
- [19] M. J. Ward, J. Wei, *Hopf bifurcation and oscillatory instabilities of spike solutions for the one-dimensional Gierer-Meinhardt model*, J. Nonlinear Science, **13**(2), (2003), pp. 209-264.
- [20] J. Wei, *On single interior spike solutions for the Gierer-Meinhardt system: uniqueness and stability estimates*, Europ. J. Appl. Math., **10**(4), (1999), pp. 353-378.

- [21] J. Wei, *Existence and stability of spikes for the Gierer-Meinhardt system*, book chapter in *Handbook of Differential Equations, Stationary Partial Differential Equations*, Vol. 5 (M. Chipot ed.), Elsevier, (2008), pp. 489-581.
- [22] J. Wei, M. Winter, *Spikes for the two-dimensional Gierer-Meinhardt system: the weak coupling case*, *J. Nonlinear Sci.*, **11**(6), (2001), pp. 415-458.

## A Numerical Source Code

```

clf;
hold off;

tlag=50;
L=1;
eps=0.06;
dt=0.0125; Tmax=500;
N=100;
maxht=zeros(1,2);
maxloc=zeros(1,2);

x=linspace(0,L,N)';
a_init=sech((x-L/2)/2/eps).^2;
h_init=1+x*0;

I=eye(N);

dx=x(2)-x(1);

Lap=-2*diag(ones(1,N))+diag(ones(1,N-1),1)+diag(ones(1,N-1),-1);
Lap(1,2)=2;Lap(N,N-1)=2;
Lap=Lap/dx.^2;

tout=0;
storelen=max(3,ceil(tlag/dt+2));
th=zeros(1,storelen);
hh=zeros(N,storelen);
ah=zeros(N,storelen);

h=h_init; a=a_init;
idx=0;
for t=0:dt:Tmax
    idx=idx+1;
    th=circshift(th, -1);
    hh=circshift(hh', -1)';
    ah=circshift(ah', -1)';

```

```

th(end)=t;
hh(:,end)=h;
ah(:,end)=a;

tprev=t-tlag;
if idx<storelen
    hT=h;
    aT=a;
else
    hT=interp1(th, hh', tprev)';
    aT=interp1(th, ah', tprev)';
end;

hp = (I-Lap)\(aT.^2/eps);

oo=aT.^2./hT-a;
%oo=a.^2./hT-a;
ap=(I/dt-eps^2*Lap)\(oo+a/dt);

h=hp;
a=ap;

if isnan(max(a))
    stop;
end;

if t>tout
    tout=tout+10;
    [t1,t2]=max(a);
    x1=a(t2-1);
    x2=a(t2);
    x3=a(t2+1);
    tt1=dx*(t2-2);
    tt2=dx*(t2-1);
    tt3=dx*(t2);
    a1=(4*x2-x3-3*x1)/(2*dx);
    a2=-(2*x2-x3-x1)/(2*(dx)^2);
    tmax=-a1/(2*a2)+tt1;
    maxht(end+1,:)= [t,t1];
    maxloc(end+1,:)= [t,tmax];
    subplot(3,1,1); plot(x,a, 'b'); hold on;plot(x,h, 'r');hold off;
    subplot(3,1,2); plot(maxloc(:,1),maxloc(:,2));
    subplot(3,1,3); plot(maxht(:,1),maxht(:,2));
    title(sprintf('t=%g',t));
    drawnow;

```

```
    end;  
end;
```